

Title	Elastic constants of polycrystalline L10-FePt at high temperatures
Author(s)	Nakamura, N.; Yoshimura, N.; Ogi, H. et al.
Citation	Journal of Applied Physics. 2013, 114(9), p. 093506-1-093506-4
Version Type	VoR
URL	https://hdl.handle.net/11094/84234
rights	This article may be downloaded for personal use only. Any other use requires prior permission of the author and AIP Publishing. This article appeared in Journal of Applied Physics, 114(9), 093506 (2013) and may be found at https://doi.org/10.1063/1.4819974 .
Note	

Osaka University Knowledge Archive : OUKA

<https://ir.library.osaka-u.ac.jp/>

Osaka University

Elastic constants of polycrystalline $L1_0$ -FePt at high temperatures

N. Nakamura,^{a)} N. Yoshimura, H. Ogi, and M. Hirao

Graduate School of Engineering Science, Osaka University, 1-3 Machikaneyama, Toyonaka, Osaka 560-8531, Japan

(Received 22 July 2013; accepted 16 August 2013; published online 3 September 2013)

Elastic constants of polycrystalline $L1_0$ FePt are studied from room temperature up to 1073 K by the electromagnetic acoustic resonance. The longitudinal-wave stiffness and the bulk modulus show intermediate values of polycrystalline Fe and Pt, but the shear modulus and Young's modulus show larger value than those of polycrystalline Fe and Pt. The Blackman diagram indicates that $L1_0$ FePt exhibits a tendency toward covalent-bond characteristic. Strong anharmonicity of the interatomic potential is confirmed from the temperature coefficient of the bulk modulus.
 © 2013 AIP Publishing LLC. [<http://dx.doi.org/10.1063/1.4819974>]

I. INTRODUCTION

$L1_0$ FePt belongs to the space group $P4/mmm$, and monoatomic layers of Fe and Pt are stacked alternately in the [001] direction.¹ $L1_0$ FePt has been attracting attention because of its large uniaxial magnetocrystalline anisotropy energy,² and numerous studies on the magnetic and structural properties have been carried out. Comparing with those properties, elastic property of $L1_0$ FePt is still unclear. Elastic constant is defined as the second order derivative of interatomic potential, and it is a fundamental parameter that informs bonding condition between atoms. Elastic constant is determined, when a material is newly found or developed because of its importance in the condensed matter physics. Experimental result is hardly reported for $L1_0$ FePt.³ Difficulty of fabrication of single crystal that is large enough to be examined is a possible reason. On the other hand, there are a few studies that calculate the elastic constants, in which the modified embedded atom method (MEAM),⁴ *ab initio* calculations using the projector-augmented wave (PAW) with the local density approximation (LDA) and the generalized gradient approximation (GGA),^{5,6} and the angular dependent analytic bond-order potential (ABOP) formalism⁵ are used. However, the calculated elastic constants vary depending on the calculation method, and the fluctuation is not small; the reported bulk modulus B ranges from 200 to 251 GPa, for instance. Experimental measurement is then indispensable for elastic constants to guide the theoretical calculation. In FePt alloys, unusual increment of elastic constants with increasing temperature has been observed for $L1_2$ Fe₃Pt,⁷⁻⁹ and temperature dependence of elastic constants of $L1_0$ FePt is of interest. In this study, the two independent elastic constants of polycrystalline $L1_0$ FePt are determined from room temperature to 1073 K.

II. EXPERIMENT

A rectangular parallelepiped, measuring $3.898 \times 2.878 \times 1.466$ mm³ in the x_1 , x_2 , and x_3 direction, respectively, was cut out of a polycrystalline Fe_{1-x}Pt_x ($x = 50.0 \pm 0.5$). The

mass density determined from dimensions and weight was 14704 kg/m³.

The elastic constants were determined by the electromagnetic-acoustic resonance (EMAR).¹⁰ EMAR determines elastic constants from resonance frequencies of mechanical free vibration of a rectangular parallelepiped specimen, in which an electromagnetic-acoustic transducer (EMAT) was used for excitation and detection of resonance vibrations. The EMAT consists of a solenoidal coil and permanent magnets. A specimen was placed in the coil, and tone bursts were applied to the coil under static magnetic field given by the permanent magnets. Interactions between the electromagnetic field induced by the coil and the static magnetic field then cause the Lorentz forces and magnetostriction forces in the specimen, and they oscillate the specimen. For an oriented rectangular parallelepiped of orthorhombic or higher elastic symmetry, we can divide free mechanical vibrations into eight groups depending on the deformation symmetry.¹¹ A_g and B_{1g} group are excited selectively by changing the direction of the static magnetic field, in this study.

We prepared two coils: one is made of copper wire covered with enamel for measurements at room temperature, and the other is made of Ni-alloy wire for measurements at high temperatures. Measurement is carried out under atmospheric pressure at room temperature and in vacuum at high temperatures. A Cantal-line heater located in the chamber supplies the heat. Temperature is measured with the thermocouple beside the specimen. Pressure during measurement was 6.4×10^{-3} Pa at most. The detailed procedures for measuring resonance frequencies at high temperatures have been given elsewhere.¹² The two independent elastic constants, longitudinal-wave modulus $C_l = \lambda + 2\mu$ and the shear modulus G , were measured between room temperature and 1073 K. λ and μ are the Lamé constant.

III. RESULTS

Figure 1 shows x-ray diffraction spectrum obtained from a surface of the rectangular parallelepiped specimen before the high-temperature experiment. Diffraction spectra were measured on other planes of the rectangular parallelepiped, and all of the diffraction peaks from $L1_0$ FePt were

^{a)}E-mail: nobutomo@me.es.osaka-u.ac.jp

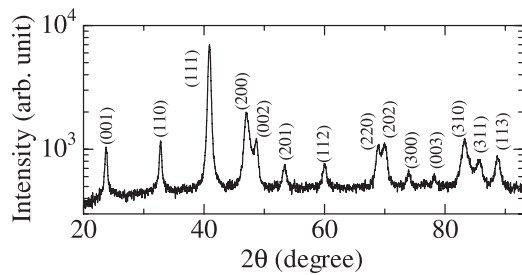


FIG. 1. X-ray diffraction spectrum of the specimen.

observed on each plane. These results confirm random orientation of $L1_0$ FePt grains, and it is valid to assume that the specimen is elastically isotropic and possesses the two independent elastic constants, C_I and G . Electron diffraction patterns were also measured after the high temperature measurement and it confirmed the $L1_0$ structure. Figure 2 shows a typical diffraction pattern. More than ten grains were surveyed and only $L1_0$ structure was observed in them.

Figure 3 shows the resonance frequencies at high temperatures. At room temperature, resonance frequencies of A_g and B_{1g} groups were measured by changing the direction of the static magnetic field. At high temperatures, the direction of the static magnetic field was fixed for A_g group. At 773 K and higher temperatures, the number of the measurable resonance frequencies decreased drastically.

Figure 4 shows temperature dependence of the elastic constants up to 1073 K. In the determination of the elastic constants, we used the dimensions and mass density measured at room temperature. Although they change with temperature, there are few studies that measured thermal expansion coefficient of $L1_0$ FePt, and the value is still ambiguous. The effect on the resultant elastic constants is estimated to be less than 1% using the reported thermal expansion coefficient,¹³ and it is negligible in the following discussion.

IV. DISCUSSION

In the high-temperature measurement, the number of measurable resonance frequencies varied at different temperatures. In a ferromagnetic material, EMAT excites resonance

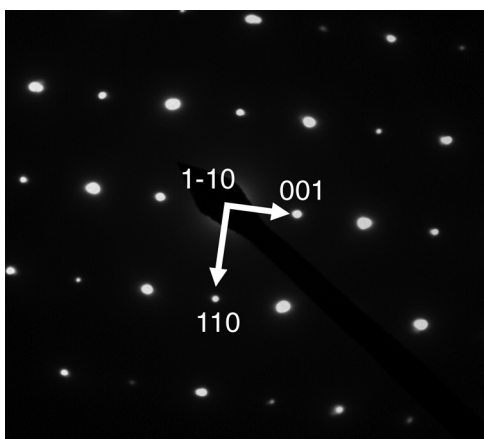
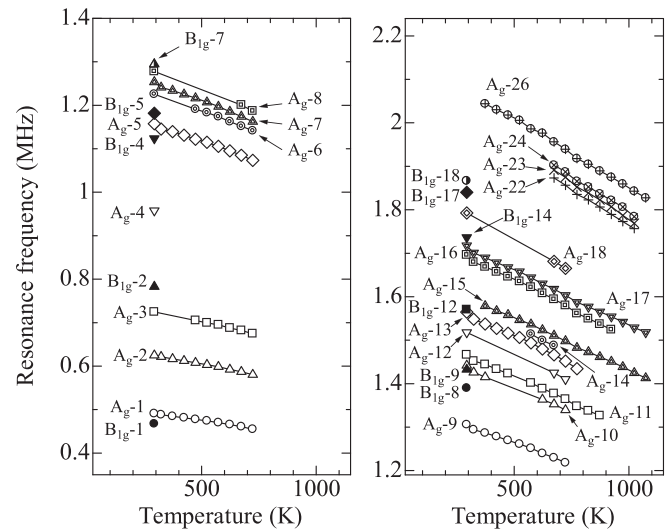


FIG. 2. The electron diffraction pattern obtained after high temperature measurement.

FIG. 3. Changes in resonance frequencies at high temperatures for low (left) and high frequency region (right). A_g - m and B_{1g} - m denote m th resonance mode of A_g and B_{1g} group, respectively.

oscillations through the Lorentz forces and the magnetostriction forces. However, contribution of the magnetostriction disappears above the Curie temperature, and the excitation efficiency becomes lower. Considering the Curie temperature of $L1_0$ FePt of 750 K,¹⁴ disappearance of some modes at 773 K and higher temperatures is explained by the disappearance of the magnetostriction.

In Table I, elastic constants measured at room temperature are compared with those measured in polycrystalline $L1_0$ FePt thin films³ together with isotropic elastic constants of Fe and Pt calculated with the Hill's average¹⁵ from elastic constants of single crystal Fe¹⁶ and Pt.¹⁷ Regarding C_I , the present value is comparable with the C_I measured in the thin films, and the value is between C_I of polycrystalline Fe and Pt. Regarding B and Poisson's ratio ν , their value of $L1_0$ FePt is also between the corresponding values of Fe and Pt, but G and E are larger than those of the polycrystalline Fe and Pt.

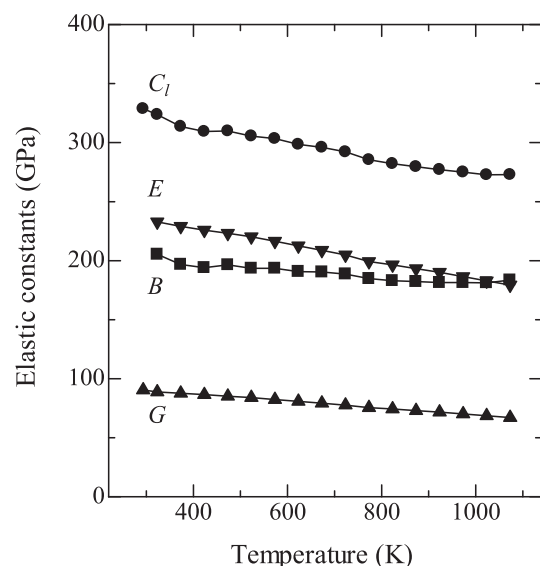
FIG. 4. Elastic constants of polycrystalline $L1_0$ FePt at high temperatures.

TABLE I. Isotropic elastic constants of Fe, $L1_0$ FePt, and Pt around room temperature. Elastic constants of $L1_0$ FePt were obtained from polycrystalline specimens and those of α -Fe and Pt were calculated from the reported elastic constants of single crystal α -Fe¹⁶ and Pt¹⁷ using the Hill's average.

	T(K)	C_l (GPa)	G (GPa)	B (GPa)	E (GPa)	ν
α -Fe ^a	300	274.8	81.5	166.2	210.1	0.289
$L1_0$ FePt ^b	293	328.8	90.5	208.1	237.2	0.310
$L1_0$ FePt ^c	Room temperature	333.0
Pt ^d	300	367.3	63.5	282.7	177.1	0.396

^aCalculated from C_{ij} in Ref. 16.

^bPresent study.

^cReference 3.

^dCalculated from c_{ij} in Ref. 17.

Blackman diagram clusters materials with similar interatomic bonding, and is independent of their absolute elastic stiffnesses. Fig. 5 shows the Blackman diagram for several materials, in which isotropic elastic constants were calculated from reported elastic constants of single crystals^{17–22} except for $L1_0$ FePt. Because Blackman diagram is defined for single crystal materials, when it is applied to the polycrystalline materials, less information is obtained. However, in Fig. 5, plots for polycrystalline metals and covalent materials appear in different regions and it still allows us to evaluate the interatomic bonding state. Polycrystalline $L1_0$ FePt shows larger G/C_l than typical metals and the plot appears close to γ -Fe. It indicates a tendency toward covalency.

A linear function $C(T) = [1 + a(T - T_{RT})]C^{RT}$ was fitted to temperature dependence of each elastic constant of $L1_0$ FePt, Fe, and Pt between 293 and 500 K, and the first-order temperature coefficients a were deduced. C denotes each elastic constant, and T_{RT} and C^{RT} denote room temperature and elastic constant at room temperature, respectively. Room temperature is 293 K for $L1_0$ FePt and 300 K for Fe and Pt. For Fe and Pt, temperature dependence of isotropic elastic constants was calculated from the elastic constants of single crystal Fe¹⁶ and Pt²³ at high temperatures using the Hill's average. The determined a is listed in Table II.

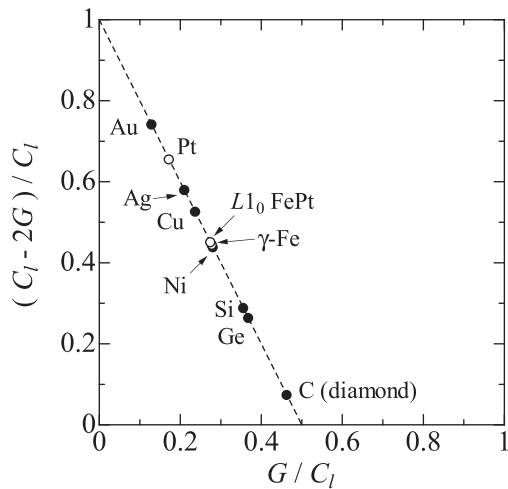


FIG. 5. Blackman diagram for polycrystalline materials. The dashed line represents elastic isotropy. C_l and G were calculated from the reported elastic constants of single crystal Au,¹⁹ Pt,¹⁷ Ag,¹⁹ Cu,¹⁹ γ -Fe,¹⁸ Ni,²⁰ Si,²¹ Ge,²¹ and C(diamond)²² except for $L1_0$ FePt.

TABLE II. Temperature coefficients of isotropic elastic constants between room temperature and 500 K ($\times 10^{-4} \text{ K}^{-1}$). Isotropic elastic constants of α -Fe and Pt at high temperatures were calculated from elastic constants of single crystal α -Fe¹⁶ and Pt,²³ respectively, using the Hill's average.

	C_l	G	B	E
α -Fe ^a	-2.2	-3.1	-1.8	-2.9
$L1_0$ FePt ^b	-3.9	-3.5	-4.2	-3.6
Pt ^c	-1.4	-2.9	-0.9	-2.7

^aCalculated from C_{ij} in Ref. 16.

^bPresent study.

^cCalculated from c_{ij} in Ref. 23.

Notable feature in the temperature coefficient of $L1_0$ FePt is the large coefficient of B . The larger coefficient indicates stronger anharmonicity of the interatomic potential of $L1_0$ FePt than Fe and Pt. The stronger anharmonicity is also confirmed in the Grüneisen parameter γ . Using the formula proposed by Ledbetter²⁴ with the temperature dependence of B and the volume thermal expansivity, γ was calculated for polycrystalline $L1_0$ FePt, Fe, and Pt; $\gamma_{\text{FePt}} = 12.3$, $\gamma_{\text{Fe}} = 3.6$, and $\gamma_{\text{Pt}} = 2.4$. The volume thermal expansivity was deduced by tripling the thermal expansion coefficient of $L1_0$ FePt,¹³ Fe,²⁵ and Pt.²⁶ The calculated γ of $L1_0$ FePt is larger than that of Fe and Pt, and it implies strong lattice anharmonicity of the interatomic potential of $L1_0$ FePt.

In Table III, the present elastic constants are compared with those obtained by the calculations.^{4–6} In calculations, thermal vibration of atom is not usually taken account, and elastic constants at 0 K are calculated. For comparison purpose, elastic constants at 0 K were estimated using the temperature coefficients in Table II and the elastic constants at room temperature in Table I, in which completely linear temperature dependence was assumed even at low temperature. Considering the general temperature dependence that temperature coefficients approach zero around 0 K, actual elastic constants at 0 K would be smaller than them. Among the calculated elastic constants, those obtained by ABOP⁵ and *ab initio* calculation (GGA)⁶ are somewhat close to the values at 0 K, though the differences between the calculated and measured elastic constants are not so small, indicating the difficulty of the calculation of elastic constants of $L1_0$ FePt.

TABLE III. Measured and calculated elastic constants of $L1_0$ FePt. C_l and G at 0 K were deduced from the temperature coefficients and elastic constants at room temperature, and B , E , and ν at 0 K were calculated from them. Isotropic elastic constants for calculations were calculated from the reported elastic constants of single crystal $L1_0$ FePt^{4–6} using the Hill's average.

	C_l (GPa)	G (GPa)	B (GPa)	E (GPa)	ν
Present study	328.8	90.5	208.1	237.2	0.310
Present study (at 0 K)	366.4	99.8	233.3	262.0	0.313
MEAM ^a	307	59	228	164	0.380
<i>Ab initio</i> calculation (GGA) ^b	310	85	196	224	0.310
<i>Ab initio</i> calculation (LDA) ^b	414	120	254	312	0.296
ABOP ^b	334	87	217	231	0.323
<i>Ab initio</i> calculation (GGA) ^c	371	112	222	288	0.283

^aCalculated from C_{ij} in Ref. 4.

^bCalculated from c_{ij} in Ref. 5.

^cCalculated from c_{ij} in Ref. 6.

V. CONCLUSIONS

Elastic constants of polycrystalline $L1_0$ FePt were determined from room temperature up to 1073 K by the electromagnetic acoustic resonance. Comparing with the elastic constants of polycrystalline Fe and Pt, the shear modulus and the Young's modulus were larger at room temperature, though the longitudinal elastic constant and the bulk modulus were between them. Furthermore, the bulk modulus showed large temperature coefficient, and it was implied that interatomic potential of $L1_0$ FePt shows strong anharmonicity.

ACKNOWLEDGMENTS

The authors would like to acknowledge the Research Center for Ultrahigh Voltage Electron Microscopy, Osaka University, and Dr. T. Sakata for the structural analysis with the transmission electron microscope.

- ¹D. E. Laughlin, K. Srinivasan, M. Tanase, and L. Wang, *Scr. Mater.* **53**, 383 (2005).
- ²D. Weller and A. Moser, *IEEE Trans. Magn.* **35**, 4423 (1999).
- ³N. Nakamura, A. Uranishi, M. Wakita, H. Ogi, M. Hirao, and M. Nishiyama, *Appl. Phys. Lett.* **98**, 101911 (2011).
- ⁴J. Kim, Y. Koo, and B. J. Lee, *J. Mater. Res.* **21**, 199 (2006).
- ⁵M. Müller, P. Erhart, and K. Albe, *Phys. Rev. B* **76**, 155412 (2007).

- ⁶N. Zotov and A. Ludwig, *Intermetallics* **16**, 113 (2008).
- ⁷G. Hausch, *J. Phys. Soc. Jpn.* **37**, 824 (1974).
- ⁸K. Tajima, Y. Endoh, Y. Ishikawa, and W. G. Stirling, *Phys. Rev. Lett.* **37**, 519 (1976).
- ⁹U. Kawald, W. Zemke, H. Bach, J. Pelzl, and G. A. Saunders, *Physica B* **161**, 72 (1989).
- ¹⁰H. Ogi, H. Ledbetter, S. Kim, and M. Hirao, *J. Acoust. Soc. Am.* **106**, 660 (1999).
- ¹¹I. Ohno, *J. Phys. Earth* **24**, 355 (1976).
- ¹²H. Ogi, S. Kai, H. Ledbetter, R. Tarumi, M. Hirao, and K. Takashima, *Acta Mater.* **52**, 2075 (2004).
- ¹³P. Rasmussen, X. Rui, and J. E. Shield, *Appl. Phys. Lett.* **86**, 191915 (2005).
- ¹⁴T. Klemmer, D. Hoydick, H. Okumura, B. Zhang, and W. A. Soffa, *Scr. Metall. Mater.* **33**, 1793 (1995).
- ¹⁵R. Hill, *Proc. Phys. Soc. A* **65**, 349 (1952).
- ¹⁶J. J. Adams, D. S. Agosta, R. G. Leisure, and H. Ledbetter, *J. Appl. Phys.* **100**, 113530 (2006).
- ¹⁷R. E. Macfarlane, J. A. Rayne, and C. K. Jones, *Phys. Lett.* **18**, 91 (1965).
- ¹⁸H. Ledbetter and S. Kim, in *Handbook of Elastic Properties of Solids, Liquids, and Gases*, edited by M. Levy, H. Bass, and R. Atern (Academic, New York, 2001).
- ¹⁹Y. Hiki and A. V. Granato, *Phys. Rev.* **144**, 411 (1966).
- ²⁰S. G. Epstein and O. N. Carlson, *Acta Metall.* **13**, 487 (1965).
- ²¹H. J. McSkimin and P. Andreatch, *J. Appl. Phys.* **35**, 3312 (1964).
- ²²N. Nakamura, H. Ogi, T. Ichitsubo, M. Hirao, N. Tatsumi, T. Imai, and H. Nakahata, *J. Appl. Phys.* **94**, 6405 (2003).
- ²³S. M. Collard and R. B. Mclellan, *Acta Metall. Mater.* **40**, 699 (1992).
- ²⁴H. Ledbetter, *Phys. Status Solidi B* **181**, 81 (1994).
- ²⁵F. C. Nix and D. MacNair, *Phys. Rev.* **60**, 597 (1941).
- ²⁶F. C. Nix and D. MacNair, *Phys. Rev.* **61**, 74 (1942).